Macromolecular Research

Article

DOI 10.1007/s13233-020-8173-2

www.springer.com/13233 pISSN 1598-5032 eISSN 2092-7673

Induced Circular Dichroism of Methylene Blue in Self-Assembled Pullulan Nanoparticles

Seo-Kyung Kim[†,1]
Soo Kyung Hwang[†,2]
Cheol Gyun Kim[1]
Hyun-Joong Kim[*,2,3]
Chong-Su Cho[*,1,2]

[1] Department of Agricultural Biotechnology, Seoul National University, Seoul 08824, Korea
[2] Research Institute of Agriculture and Life Sciences, Seoul National University, Seoul 08824, Korea
[3] Program in Environmental Materials Science, Department of Agriculture, Forestry and Bioresources, Seoul National University, Seoul 08824, Korea

Received May 12, 2020 / Revised October 23, 2020 / Accepted October 31, 2020

Abstract: This study reports self-assembled pullulan nanoparticles (PUNPs) obtained by the diafiltration method after dissolving phthalic pullulan in dimethylformamide, which was prepared by esterification between the primary hydroxyl groups of the pullulan and carboxylic acids of phthalic anhydride. The morphologies of the PUNPs observed by transmission electron microscopy (TEM) were spherical shapes. The particle sizes of the PUNPs measured by dynamic light scattering (DLS) were around 75.3 nm with -49.32 mV zeta potential. The ordered structure of pullulan measured by circular dichroism (CD) spectroscopy and X-ray diffraction (XRD) was enhanced by the formation of self-assembled polymeric NPs. Methylene blue (MB) used in tissue imaging agent was loaded into PUNPs *via* ionic bonding of cationic MB and anionic PUNPs, the CD of MB was induced in the PUNPs in the range of 500-700 nm whose crossing point matched λ_{max} in the UV region of MB.

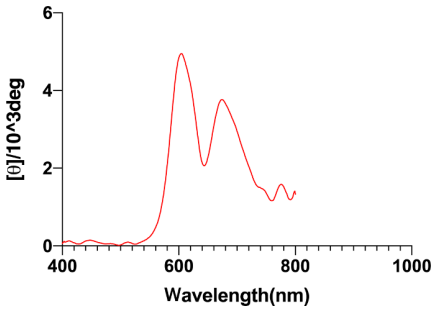

Keywords: nanoparticle, methylene blue, pullulan, induced circular dichroism.

1. Introduction

Polymeric nanoparticles (NPs) have been attracted in many fields because they have unique optical, electrical, magnetic and biomedical properties due to their wide surface area and easy control of diverse surface chemistry.[1] Also, they can deliver chemical drugs, genes, proteins, and optical imaging agents to the desired place according to the specific biological or external stimuli.[2] Especially, they have been used to overcome cellular barriers for delivering hydrophobic chemical drugs and biomacromolecules into the cells because they can be easily internalized with cellular membranes through the endocytosis.[3] Furthermore, they can be applied for the delivery of optical imaging agents because the optical imaging as the non-invasive methods of diagnostic area enables observation of the distribution and distribution of used drugs in a short time with high resolution.[4]

Among processing of several polymeric NPs, polymeric NPs are easily formed by the self-assembly of amphiphilic polymers composed of hydrophilic groups and hydrophobic ones due to the hydrophobic interaction of hydrophobic groups in the inner cores of the polymeric NPs.[5] The polymeric NPs have been used to deliver hydrophobic anticancer drug,[6] proteins[7-9] and imaging agents.[10-12]

The optical activity of molecules induced by a chiral environment has received much attention because it is very important in the biopharmacology and biochemistry.[13,14] Generally, the induction of circular dichroism (CD) occurred through the interaction of guest molecules, such as dyes,[15,16] diazirin chromophore,[17] and bilirubin[18] with the host molecules, such as cyclodextrin,[18] DNA[19] and polypeptides.[20,21] The host-guest interaction was formed by covalent linking or physical bonding and the interaction exhibited an induced CD (ICD) in the UV or visible region of the guest molecules.[22]

Pullulan consisted of three glucose moieties connected by an α-1,4 glycosidic bond can be specifically internalized by liver cells through asialoglycoprotein receptors (ASGPRs).[22] The pullulan NPs have been used to deliver drugs[23] and siRNA in the liver cells.[24]

In this study, we are aimed to report on the ICD of methylene blue (MB) dye as the guest in the self-assembled pullulan NPs as the host. It is of particular interest to study the ICD of the MB used in tissue imaging agent due to its properties such as staining, slight fluorescent in the mean infrared region, and it has been approved by FDA.[25] Especially, the ICD of MB in the pullulan NPs can be used for liver tissue imaging agent because of specific interaction of pullulan with ASGPRs.

2. Experimental

2.1. Materials

Pullulan was provided by Shandong Freda Biotechnology Co., Ltd (Shandong, China). The other chemicals were provided by Sigma-Aldrich (St. Louis, MO, USA).

Acknowledgments: We would like to thank Prof. J.P. Kim at Seoul National University to providie MB in this study. Also, This research was supported by Basic Science Research Program through the National Research Foundation of Korea(NRF) funded by the Ministry of Education (NRF-2020R1I1A1A01053275).

***Corresponding Authors:** Hyun-Joong Kim (hjokim@snu.ac.kr), Chong-Su Cho (chocs@snu.ac.kr)
[†]These authors contributed equally to this work.

2.2. Synthesis of phthalic pullulan (PP) and preparation of PUNPs

Before preparation of PUNPs, PP was synthesized by a previously described method.[26] One gram of pullulan and 0.1 mol.% dimethyl amnopyridine (DMAP) as a catalyst were dissolved in 10 mL of dimethyl formamide (DMF), and then 2.64 g of phthalic anhydride (9 times molar ratio) per pullulan was added to the above solution. The reaction was performed at 54 °C for 48 h under nitrogen. After the reaction, the above reactant was firstly dialyzed in DMF to remove unreacted phthalic anhydride and then in distilled water at 4 °C for 48 h. The unreacted pullulan was removed by ultra-centrifugation of dialyzed sample. After centrifugation, the supernatant was freeze-dried. Finally, the PUNPs were prepared by the dialysis tubing (12,000, molecular weight cutoff) in distilled water after dissolving the PP in DMF at 4 °C for 24 h, and then the PUNPs were freeze-dried and stored at -20 °C until use.

2.3. Confirmation of synthesis of PP and characterization of PUNPs

The synthesis of PP and content of phthalic groups in the PP was confirmed by 600 mHz ^{1}H-nuclear magnetic resonance (NMR) spectroscopy (AVANCE 600, Bruker, Germany). The morphologies of PUNPs were observed by transmission electron microscopy (TEM)(LIBRA 120, Carl Zeiss, Germany). The particle sizes of PUNPs were measured by a dynamic light scattering (DLS) spectrophotometer (DLS-7000, Otsuka Electronics, Japan). The zeta potential of the PUNPs was measured by an electrophoretic light scattering (ELS) spectrophotometer (ELS-8000, Otsuka Electronics, Japan).

2.4. Preparation of MB-loaded PUNPs

Thirty mg of PP dissolved in 10 mL DMF was dialyzed in distilled water by dialysis tube (molecular weight cut-off of 12,000-14,000) for 24 h at 4 °C and freeze-dried. And then, 0.05 wt.% of MB dissolved in water was added into 1 wt.% of PUNPs dispersed in water.

The loading content and loading efficiency of MB in the PUNPs were calculated using the following equations:

Loading content (%)=amount of MB in the PUNPs/amount of MB-loaded PUNPs X 100%

Loading efficiency (%)=amount of MB in the PUNPs/amount of MB initially used X 100%

2.5. CD and UV/Vis absorption spectroscopy measurement

CD spectra were measured by Chirascan plus (Applied photophysics, UK) at room temperature by a quartz cell with an optical pathlength of 1mm. All spectra were accumulated three times of 1 nm at a scan speed of 50 nm/min. The ICD was obtained as the CD of MB-loaded PUNPs minus the CD of MB and PU measured at the same wavelength and expressed as ellipticity in milidegrees.[27] The Vis spectra were measured by an UV/Vis spectrometer (Cary100, Agilent, USA) at room temperature.

2.6. Measurement of wide angle X-ray diffraction (WAXRD) and small angle X-ray spectrometer (SAXS)

The WAXRD patterns were obtained by a D8 ADVANCE diffractometer (Bruker DAVINCI, Germany) equipped with a Cu radiation source with a wavelength (λ) of 1.5418 Å. The WAXS diffractograms were measured at room temperature at 40 kV , 40 mA, and at a scan speed of 0.5°/sec in the range of 10-70° 2θ range, where θ is the angle of incidence of X-ray beam on the sample. Also, the SAXS spectroscopy was measured using a 1.54189 Å synchrotron X-ray beam (System model : Small Angle X-ray Scattering Spectrometer, Xenocs, France). The sample (bulk state)-to-detector distance was 300 nm and the SAXS data was acquired for 600 s under ambient conditions.

3. Results and discussion

3.1. Synthesis of PP and characterization of PUNs

The reaction scheme of PP synthesis is shown in Figure 1. The synthesis of PP was confirmed by measurement of ^{1}H-NMR spectroscopy as shown in suppl. Figure 1. It was found that peaks of 7.4-7.7 ppm assigned to the phthalic acid protons, and peaks of 4.68 and 5 ppm assigned to the sugar protons (C_1 position of α-1,6 and α-1,4 glycosidic bonds, respectively) as described by Tao et al.[28] appeared in the NMR spectrum of PP, the suggestion of successful synthesis of PP through the esterification between the primary hydroxyl groups of the pullulan and the carboxylic acids of phthalic anhydride. The degree of substitutions (DS) of phthalic groups in the PP was estimated by determining the ratio of phthalic acid protons to sugar ones. The results indicated that the DS in the PP was 62.5 mol.%. The morphologies of PUNPs prepared by self-assembled polymeric NPs after conjugation of phthalic anhydride as the hydrophobic groups to hydroxyl groups in pullulan through hydrophobic interactions were observed as spherical shapes and sized between 20 and 30 nm due to the dry state whereas the particle sizes of the MB-loaded PUNPs ranged from 30-50 nm with the more irregular round spherical shapes due to the ionic interaction of positive charge of MB and negative charge of PUNPs as shown in Figure 2(A) and (B), respectively. The particle sizes of PUNPs measured by cumulants results of DLS were 75.3 nm with polydispersity index of 0.256 as shown in Figure 3 whereas the particle sizes of PUNPs measured by volume distribution of DLS were 46.4 nm with 67. 9 nm of standard deviation (data not shown). Also, the surface charge of the PUNPs measured by an electrophoretic light scattering (ELS) was -49.32 mV as shown in Figure 4, the suggestion of negative zeta potential due to the unreacted carboxyl groups in the PP.

3.2. Diffractometry of WAXRD and SAXS

XRD patterns for pullulan and PUNPs are shown in Figure 5. As shown in Fig., the XRD pattern of pullulan exhibits a peak at 2θ value of about 18.4° that corresponds to d-spacing of 0.24 nm due to the triple-helical pitch.[29] On the other hand, the XRD patterns of PUNPs exhibit peaks at 2θ values of about 18.4°, 27.1°, and 41.8° that correspond to d-spacing of 0.24, 0.17, and 0.12 nm,

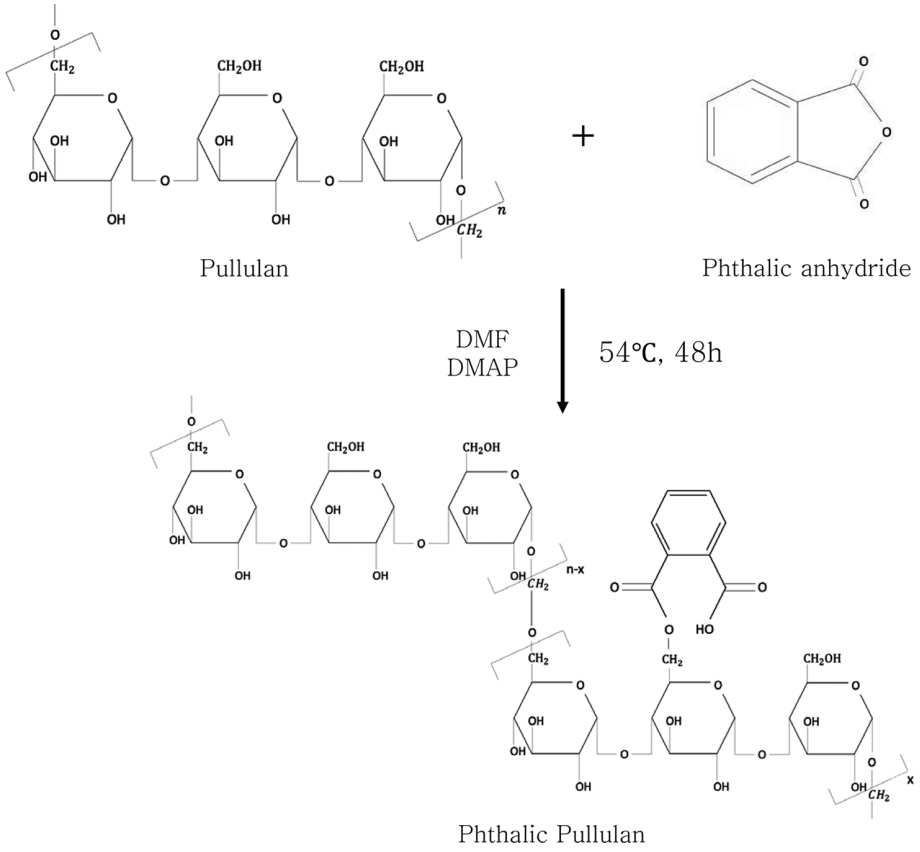

Figure 1. Chemical reaction scheme of PP synthesis.

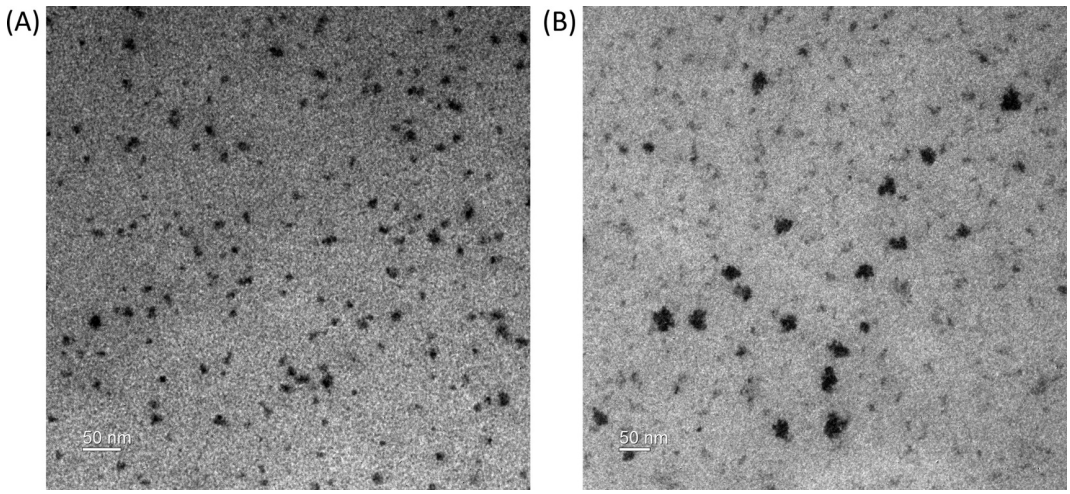

Figure 2. Morphologies of PUNPs (A) and MB-loaded PUNPs (B) observed by TEM.

respectively. The weak peak at 18.4° corresponds to the triple-helical pitch and the remaining peaks at 27.1° and 41.8° ascribed to regular nanosized structures due to the formation of self-assembled PUNPs.[30] When we checked the XRD patterns for MB-loaded PUNPs, there were no peaks of the MB in the MB-loaded PUNPs except the peaks of PUPBs (data not shown), suggesting that loaded MB in the PUNPs became amorphous state after loading in the PUNPs although there were several sharp peaks of MB itself due to the crystalline state.

SAXS diffraction pattern for PUNPs is shown in Figure 6. As shown in Fig., a SAXS diffraction peak was observed at q=4.6 nm^{-1} for PUNPs, which corresponds to a d-spacing of 1.36 nm, as a similar pattern with the triple-helical pitch of schizophyllan polysaccharide[30] possibly ascribable to the formation self-assembled PUNPs although a SAXS diffraction peak was not observed for pullulan (data not shown).

3.3. Measurement of UV and CD

Figure 7 shows UV spectra of the MB (A) and MB-loaded PUNPs.

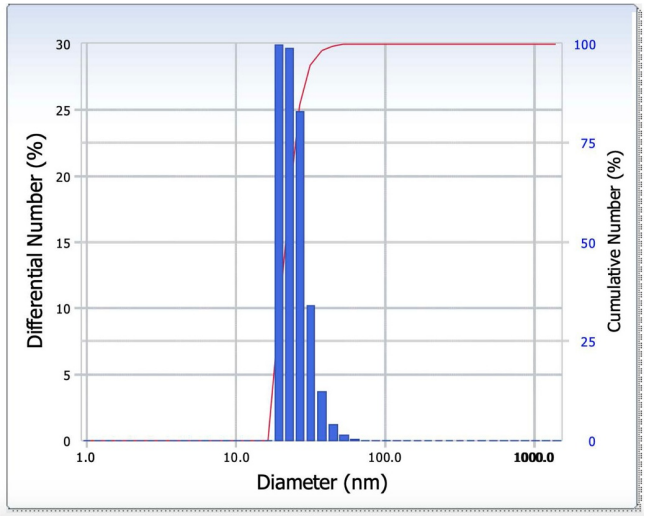

Figure 3. Particle sizes of PUNPs measured by DLS.

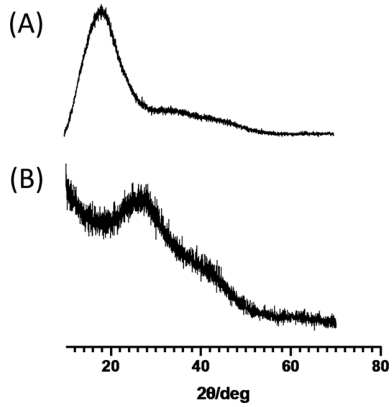

Figure 5. XRD patterns of pullulan (A) and PUNPs (B) measured by WAXRD.

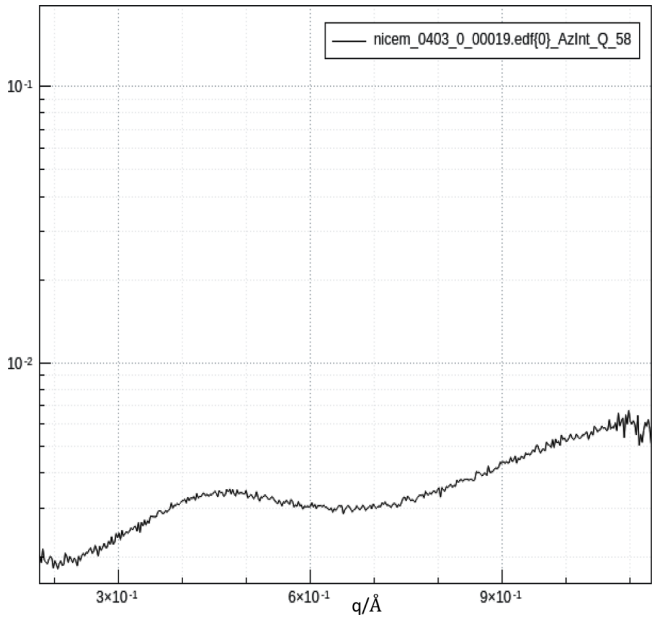

Figure 6. SAXS diffraction pattern of PUNPs.

As shown in the Figure 7(A), a characteristic MB monomer peak at λ_{max} 664.0 nm with a shoulder peak at 619.3nm attributed to the formation H-aggregates of the dye.[31] On the other hand, a characteristic H-aggregates of MB (λ_{max}=607.0nm) with a shoulder peak at λ_{max} 671.0 nm of MB monomer peak after loading of MB into the PUNPs was obtained as shown in Figure 7(B) due to the ionic and hydrophobic bondings between MB and PUNPs.

Figure 8 shows CD spectra of pullulan itself (A) and PUNPs (B) according to temperature in water. As shown in Figure 8(A), the pullulan exhibited a very weak negative absorption arised from coupling of C-O-C ether chromophores, leading to negative residual ellipticity with a maximum at 187 nm for alpha-helices[32] although the alpha-helicity of the pullulan decreased as temperature was increased with a red-shift of the maximum due to the breakdown of the H-bonding in the pullulan. On the other hand, the PUNPs exhibited two negative ellipticities at 194 nm

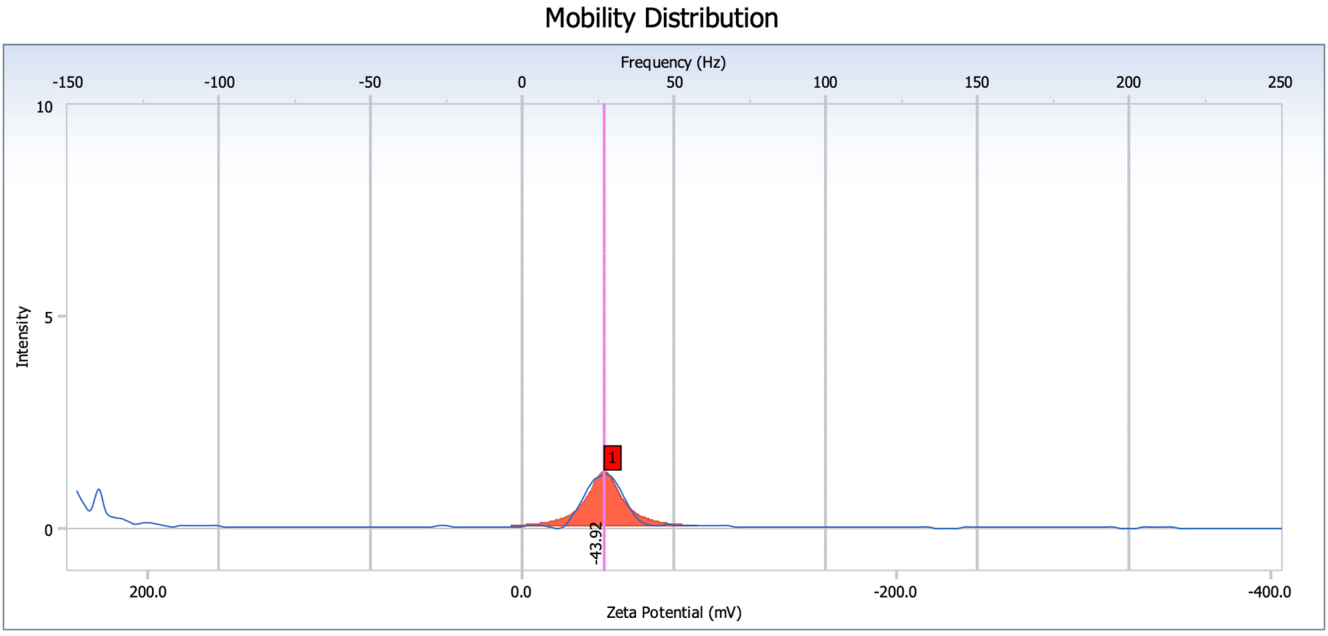

Figure 4. Zeta potential of PUNPs.

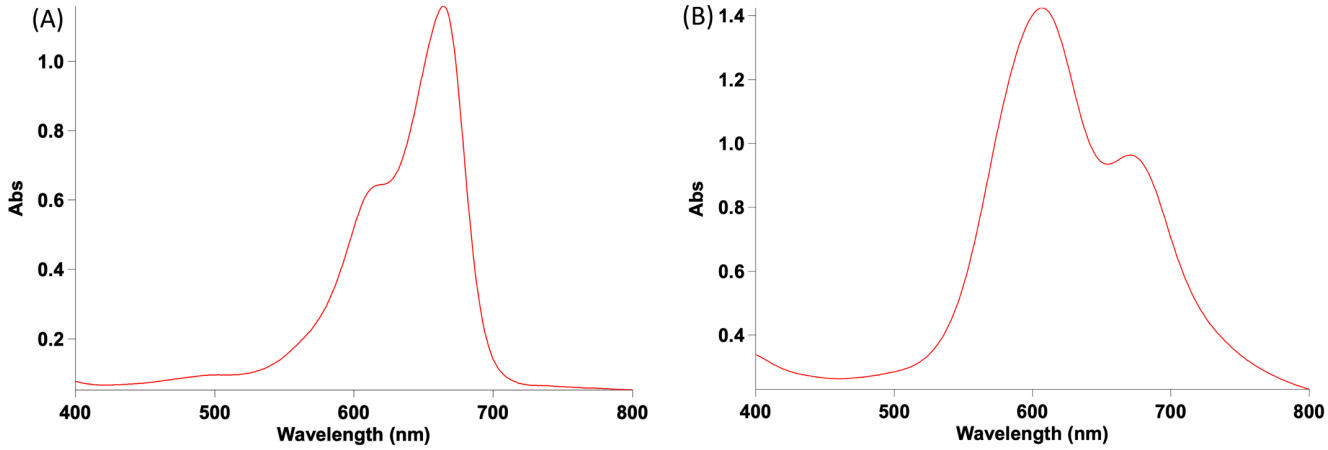

Figure 7. UV spectra of MB (A) and MB-loaded PUNPs (B).

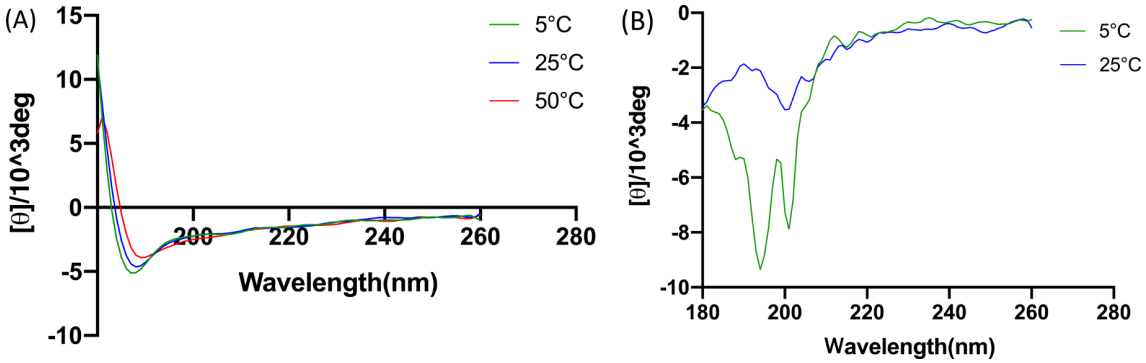

Figure 8. CD spectra of pullulan (A) and PUNPs (B) in water according to temperature.

for alpha-helices and 201 nm for beta-sheets-like structure although the alpha-helices in the PUNPs disappeared at 25 °C and 50 °C (data not shown), suggesting that conformational changes pullulan occurred from alpha-helices to beta-sheets by the formation of self-assembled polymeric NPs. These behaviors are very similar with the results of Forget *et al.*.[33] They reported that carboxylation of agarose exhibited a new ellipticity at 203 nm with a red-shift from 191 nm due to promotion of reorganization of the chains leading to a new secondary structure in agarose in addition to the alpha-helices although beta-sheet structure of the agarose was affected by temperature.[33]

Figure 9 shows CD spectrum of the MB-loaded PUNPs. The result indicated that two strong bands appeared in the CD spectrum at around UV absorption maximum of MB shown in the UV spectrum, the indication of ICD of the MB by chiral PUNPs, suggesting that the observed ICD spectrum of the MB was matched with its UV absorption spectrum precisely.

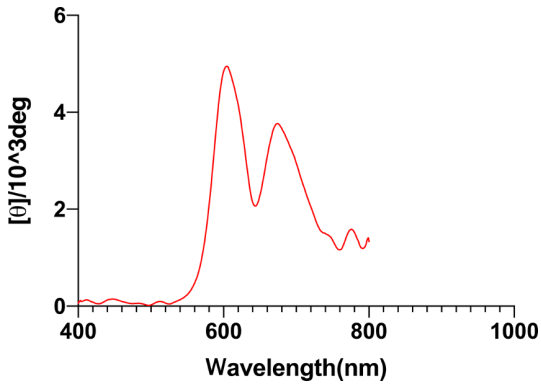

Figure 9. CD spectrum of MB-loaded PUNPs in water at 25 °C.

4. Conclusion

The regular nanosized structures appeared in the PUNPs and conformational change from alpha helices structure to beta-sheet-like one of pullulan occurred by the formation of self-assembled polymeric NPs through hydrophobic interaction of incorporated hydrophobic groups in the pullulan. MB was loaded into the PUNPs through ionic and hydrophobic bondings between MB and PUNPs. The CD of the MB was induced by the chiral microenvironment of PUNPs. Imaging of MB-loaded PUNPs for liver tissue therapy will be reported in the future.

Supporting information: ^{1}H-NMR spectrum of PP was shown in supplementary figure. The materials are available *via* the Internet at http://www.springer.com/13233.

References

(1) N. G. Portney and M. Ozkan, *Anal. Bioanal. Chem.*, **384**, 620 (2006).
(2) R. A. Petros and J. M. DeSimone, *Nat. Rev. Drug Discov.*, **9**, 615 (2010).
(3) M. Elsabahy and K. L. Wooley, *Chem. Soc. Rev.*, **41**, 2545 (2012).

(4) M. S. Murahari and M. C. Yergeri, *Curr. Pharm. Des.*, **19**, 4622 (2013).
(5) W.-S. Kim, J.-Y. Lee, B. Singh, S. Maharjan, L. Hong, S.-M. Lee, L.-H. Cui, K.-J. Lee, G. Kim, C.-H. Yun, S.-K. Kang, Y.-J. Choi, and C.-S. Cho, *Sci. Rep.*, **8**, 5878 (2018).
(6) W. Im and H. S. Kim, *Tissue Eng. Regen. Med.*, **16**, 213 (2019).
(7) K. J. Kim, M. S. Choi, J. H. Shim, and J. W. Rhie, *Tissue Eng. Regen. Med.*, **16**, 395 (2019).
(8) S.-Y. Yoon, S.-K. Kang, H.-B. Lee, S.-H. Oh, W.-S. Kim, H.-S. Li, J.-D. Bok, C.-S. Cho, and Y.-J. Choi, *Tissue Eng. Regen. Med.*, **17**, 33 (2020).
(9) K.-W. Ko, Y.-I. Yoo, J. Y. Kim, B. Choi, S.-B. Park, W. Park, W.-K. Rhim, and D. K. Han, *Tissue Eng. Regen. Med.*, **17**, 155 (2020).
(10) C. G. Yang, G. K. Park, E. J. McDonald, and H. S. Choi, *Tissue Eng. Regen. Med.*, **16**, 433 (2019).
(11) J. S. Jung, D. Jo, G. Jo, and H. Hyun, *Tissue Eng. Regen. Med.*, **16**, 443 (2019).
(12) S. Pillarisetti, S. Uthaman, K. M. Huh, Y. S. Koh, S. Lee, and I.-K. Park, *Tissue Eng. Regen. Med.*, **16**, 451 (2019).
(13) T. Miyagawa, M. Yamamoto, R. Muraki, H. Onouchi, and E. Yashima, *J. Am. Chem. Soc.*, **129**, 3676 (2007).
(14) T. Nishimura, S. Shinoda, H. Tsukube, *Chirality*, **14**, 555 (2002).
(15) N. Yoshida, H. Yamaguchi, and M. Higashi, *J. Chem. Soc., Perkin Trans.* **2**, 2507 (1994).
(16) V. Buss, *Angew. Chem. Int. Ed.*, **30**, 869 (1991).
(17) D. Krois and U. H. Brinker, *J. Am. Chem. Soc.*, **120**, 11627 (1998).
(18) D. A. Lightner, J. K. Gawronska, and K. Gawronska, *J. Am. Chem. Soc.*, **107**, 2456 (1985).
(19) D. J. Owen, D. VanDerveer, and G. B. Schuster, *J. Am. Chem. Soc.*, **120**, 1705 (1998).
(20) T. W. Chung, B. J. Kim, S. Y. Park, T. Akaike, J. W. Nah, and C. S. Cho, *Macromolecules*, **33**, 8921 (2000).
(21) T. W. Chung, J. W. Nah, T. Akaike, Y. H. Park, and C. S. Cho, *Polymer*, **41**, 6415 (2000).
(22) J. Jo, M. Yamamoto, K. Matsumoto, T. Nakamura, and Y. Tabata, *J. Nanosci. Nanotechnol.*, **6**, 2853 (2006).
(23) Y. Tabata, Y. Matsui, K. Uno, Y. Sokawa, and Y. Ikada, *J. Interferon Cytokine Res.*, **19**, 287 (1999).
(24) I. Kanatani, T. Ikai, A. Okazaki, J.-I. Jo, M. Yamamoto, M. Imamura, A. Kanematsu, S. Yamamoto, N. Ito, O. Ogawa, and Y. Tabata, *J. Control. Release*, **116**, 75 (2006).
(25) A. Matsui , E. Tanaka, H. S. Choi, V. Kianzad, S. Gioux, S. J. Lomnes, and J. V. Frangioni, *Surgery*, **148**, 78 (2010).
(26) L. Hong, W.-S. Kim, S.-M. Lee, S.-K. Kang, Y.-J. Choi, and C.-S. Cho, *Front. Microbiol.*, **10**, 142 (2019).
(27) M.-K. Yoo, M.-Y. Park, S.-W. Lee, Y.-J. Choi, I.-K. Park, and C.-S. Cho, *J. Nanosci. Nanotechnol.*, **10**, 3551 (2010).
(28) X. Tao, Y. Xie, Q. Zhang, X. Qiu, L. Yuan, Y. Wen, M. Li, X. Yang, T. Tao, M. Xie, Y. Lv, Q. Wang, and X. Feng, *Nanomaterials (Basel)*, **6**, 165 (2016).
(29) H. Kono, N. Kondo, T. Isono, M. Ogata, and K. Hirabayashi, *Int. J. Biol. Macromol.*, **154**, 1382 (2019).
(30) D. B. Kony, W. Damm, S. Stoll, W. F. van Gunsteren, and P. H. Hunenberger, *Biophys. J.*, **93**, 442 (2007).
(31) M. Karmakar, M. Mahapatra, A. Dutta, P. K. Chattopadhyay, and N. R. Singha, *Int. J. Biol. Macromol.*, **102**, 438 (2017).
(32) E. R. Arndt and E. S. Stevens, *Carbohydr. Res.*, **303**, 73 (1997).
(33) A. Forget, J. Christensen, S. Lüdeke, E. Kohler, S. Tobias, M. Matloubi, R. Thomann, and V. P. Shastri, *Proc. Natl. Acad. Sci. U.S.A.*, **110**, 12887 (2013).

